Intra-Pixel Sensitivity in NIR Detectors for NGST

Utkarsh Sharma[a], Donald F. Figer[a,b], Bernard J. Rauscher[a] Michael W. Regan[a], Louis Bergeron[a], Jesus Balleza[a], Robert Barkhouser[b], Russ Pelton, Mike Telewicz, Paul Stemniski, S. Kim, Gretchen Greene[a], Stephan McCandliss[b], Anand Shivaramakrishanan[a] , Tom Reeves[b], H. S. Stockman[a]

ABSTRACT

Intra-Pixel Sensitivity (IPS) is defined as the spatially varying response of the pixel to incoming flux. IPS plays a crucial role when the Point-Spread Function (PSF) is critically, or under-, sampled. Variations in IPS lead to photometric and astrometric errors. The Next Generation Space Telescope (NGST) requires high quality photometry and astrometry, so an accurate estimation of the IPS function is necessary for a successful NGST mission. Photo-electrons generated in a pixel may be detected in the depletion region (detection of the flux) of the same pixel, or might diffuse and end up in the microstructure of the detector, the electric field distribution therein, wavelength of the incident radiation, and diffusion processes of the excess charge carriers generated determines the IPS function of a pixel that can vary from pixel to pixel. The total detected flux is proportional to the convolution of the PSF and the IPS function. If we approximate the profile of the PSF, then the problem of determining the IPS function reduces to deconvolving using the experimentally obtained Sensitivity variation profile and the calculated PSF. We aim to obtain a highly undersampled PSF, scan it over a single pixel on a grid of 10 x 10 points, and retrieving IPS function using deconvolution. We present our results, experiment design, and the scope of further work, using an NGST detector, to estimate the IPS function at various wavelengths.

1. INTRODUCTION

The Next Generation Space Telescope (NGST) aims to detect the faintest and earliest light to study the origins of the universe. IR astronomy offers many advantages over conventional astronomy as, it is effective in imaging of cold and older stars, and IR waves being much more penetrative than visible or UV light, can reveal processes in star forming regions, which are typically enshrouded in dust and gas clouds. Hence highly sensitive near-infrared (NIR) detectors will play a key role to probe origins of galaxies and stars since their light is redshifted to IR spectrum by cosmological expansion.

High precision astrometry (accurate position determination) and photometry would be required for meeting the requirements set by NGST, which might suffer from systematic errors in the case of undersampled images unless the accurate intra-pixel sensitivity function is derived. The effects of Intra-pixel varying response might be neglected for well sampled images, but its effects become quite prominent and might lead to information loss while detecting faint undersampled images, or determining accurate Point Spread Functions (PSF, defined as the response of the imaging system to a point source input). Various techniques, such as using, a bias dark frame, or a flat field calibration, have been developed and employed to rectify pixel to pixel variations in a solid state detector. However all these corrective techniques assume uniform sensitivity within a single pixel, and hence don't apply an Intra-pixel sensitivity correction. Hubble Space Telescope (HST) has a unique capability of producing sharp imaging, which is very crucial for accurate astrometry. In HST images, most of the objects are relatively isolated point-source stars. The undersampled images obtained with the Planetry Camera (PC) and the Wide Field Camera (WFC) in the HST run high risk of erroneous astrometry leading to pixel-phase error, an error that is related to the location of a star with respect to pixel boundaries. Differential astrometry techniques require the accurate knowledge of the IPS function in order to remove this pixel-phase error [1].

Images taken by the WFPC2 CCDs inthe HST shows that the detected stellar flux can vary by a few percent as a function of position within the pixel [2]. Photometric corrections and effective PSF reconstruction techniques based on dithered set of data for undersampled images have been suggested but are still inadequate for severly undersampled images [3,4]. Non uniform intra-pixel sensitivity profiles of front as well as back illuminated CCD's were obtained in a high precision experiment by scanning a highly undersampled image of a laser spot [5,6,7]. All these experiences with astronomical imaging and experimentally verified IPS variations in CCD's led us to conclude that IPS could be a crucial factor in high precision astronomy using NIR detectors.

In this paper we discuss the physical factors that lead to intra-pixel sensitivity, followed by a description of the experimental setup for the determining the IPS of prototype NIR detectors for NGST. Finally, we present data and preliminary results, followed by the conclusion.

2. THE ORIGIN OF INTRA PIXEL SENSITIVITY

After detector material absorbs photons, the resultant photogenerated electron-hole pairs diffuse randomly through the substrate; holes that reach the edge of the depletion region are preferentially swept by the electric field in the depletion region and thereby counted as signal charge. Electron-hole pairs generated by incident radiations may be governed by one of these three processes :

a). Holes being collected in the depletion region of the pixel where they were generated (detection of signal)
b). Holes diffusing in lateral direction and ending up being detected in the neighboring pixels (Crosstalk)
c). Electron-hole pairs recombining before holes can make it to the depletion region (Loss of information)

Intra-Pixel Sensitivity (IPS) is defined as the spatially varying response of the pixel to incoming flux and we can see that spatial response of the pixel will depend on what is the weighted probability of each process for a new electron-hole pair generated. The detector/physical parameters, which can affect these processes and thus lead to variations in the IPS are [8]:

a). Absorption coefficient as a function of wavelength.
b). Thickness of the detector substrate as well as the detector geometry (pixel size etc.).
c). Diffusion length of excess carriers.
d). Rear or front illumination.

The absorption coefficient determines the concentration of electron-hole pair generation as a function of depth. A larger absorption coefficient implies lesser lateral diffusion (hence lesser crosstalk). Electron-hole pairs generated deep within the substrate are subject to stronger lateral diffusion, nevertheless their chances of getting lost via recombination are less in case of rear illumination, as they are generated much closer to the depletion region. However, in case of front illumination, the crosstalk will increase with the increase in wavelength because the longer wavelengths will get absorbed further inside the detector, where the lateral diffusion will be stronger. Thickness of the detector is normally tailored so as to obtain maximum efficiency. A thicker detector might have higher quantum efficiency, so as to absorb all the incoming flux, but it might result in more electron-hole pairs being detected in adjoining pixels. Diffusion length could be a critical factor, as well, if its dimensions are comparable to the thickness of the detectors. A longer diffusion length can increase sensitivity but at the same time it can lead to an increase in the crosstalk. Hence there is a tradeoff in various aspects of efficiency of the detectors and the detector parameters should be chosen so as to optimize the overall efficiency.

3. SIGNAL RESPONSE OF A PIXEL : THEORETICAL FORMULATION

Ideally, the IPS function should have constant value within the boundaries of the pixel (i.e. uniform spatial sensitivity) and zero outside (i.e. zero crosstalk), and then only can we can assume that the detected signal is directly proportional to the flux incident on the pixel. However it is not so in reality, and in order to investigate the effects of sub-pixel sensitivity variations, it will be convenient to define an intra-pixel sensitivity (IPS) function (also known as pixel response function, PRF), and point spread function (PSF), which is defined as the response of the telescope and camera optics to a point source object. The signal response of a given pixel N(i,j) as a function of the spatial position of the center of the PSF(x,y), is given by the convolution of the IPS(i,j) and PSF functions :

$$N(i,j,x,y;\lambda) = \int_{-\infty}^{\infty}\int_{-\infty}^{\infty} PSF(x_1 - x, y_1 - y;\lambda)\, IPS(i,j,x_1,y_1;\lambda)\, dx_1 dy_1 \qquad (1)$$

We can also define IPS as the signal response when the PSF is a δ-function (infinitesimally small) image of a point source; in practice, the PSF is limited by the diffraction due to optics. The IPS term completely defines the imaging characteristics of the detector arrays, it includes not only the sensitivity response as a function of location within the pixel, but also the crosstalk due to diffusion of photogenerated electron hole pairs. To be more specific :

1. If the coordinates (x_1, y_1) are within the pixel (i,j), then the IPS represents the map of the spatial pixel sensitivity, i.e., the response of the pixel as a function of position of the source on it.
2. Whereas if the coordinates (x_1, y_1) are outside the boundary of the pixel (i,j), then the IPS represents the map of the cross-pixel response, i.e., the response of the pixel as a function of position of the source on a neighboring pixel.

Since the PSF can't be a spatial δ-function, we need to deconvolve eq 1 to retrieve the actual IPS function. If we assume that we know the PSF, then we are left with one unknown function to solve, which is IPS. The problem of finding the IPS function then reduces to solving the Fredholm integral equation of the first kind [9]. One of the most common methods is to use collocation method for linear integral equations [10]. We assumed a gaussian profile for the PSF, with a diffraction limited Full Width Half Maximum (FWHM). We simulated the signal a pixel with a given IPS function would produce when illuminated by a Gaussian PSF centered at various points within the pixel. We then inverted the data to recover the input IPS function in the presence of Poisson noise. We simulated scanning a PSF of constant intensity (with poisson noise) over a pixel on a grid of 10 x 10 points, and calculated the pixel output at each point, solving for the IPS function values at each point. As long as the width of PSF is small, this numerical method of IPS retrieval works well but it starts failing to converge as the width of PSF increases. Our simulation results show that the inferred IPS function starts getting erratic as the width of the PSF increases (Fig 1). Hence we conclude that one of the essential requirements to determine an accurate IPS function is to obtain a highly undersampled PSF.

4. EXPERIMENTAL SETUP

The IR detector are enclosed in the IDTL Dewar system [11], which is cryogenically cooled in two stages, at ~10K (for detectors) and ~60 K (for detector housing) respectively. The optical system, which is mounted inside the dewar, consists of an f/10 1:1 reimaging offner relay, in conjunction with an f/1.5 focal reducer to provide subpixel imaging (Fig 2). The lateral and longitudinal demagnification factors of the optical system are 7 and 49 respectively. The focal reducer is made of diamond machined ZnS. It has four independent prescriptions on its two surfaces, with portions of both surfaces diamond coated to induce reflections back in to the material. Note that rays are perpendicular with respect to the lens surfaces at both places where there is a change in refractive index, i.e. the lens is achromatic. The H1R detector (1024x1024 18 μm square pixel) was operated at temperatures at temperatures near 35 K. The source object is a pinhole mounted on the three axis programmable translational stage with the resolution of 0.075 μm, illuminated by a uniform spatial profile, at the plane of the pinhole, of a white light source with tunable intensity. Various filters (J,H,K,L,M, and PK50) can be used to obtain the required bandwidth by rotating the cryogenic filter wheel. The Dewar is mounted on an optical air table to minimize the vibrations from the ground.

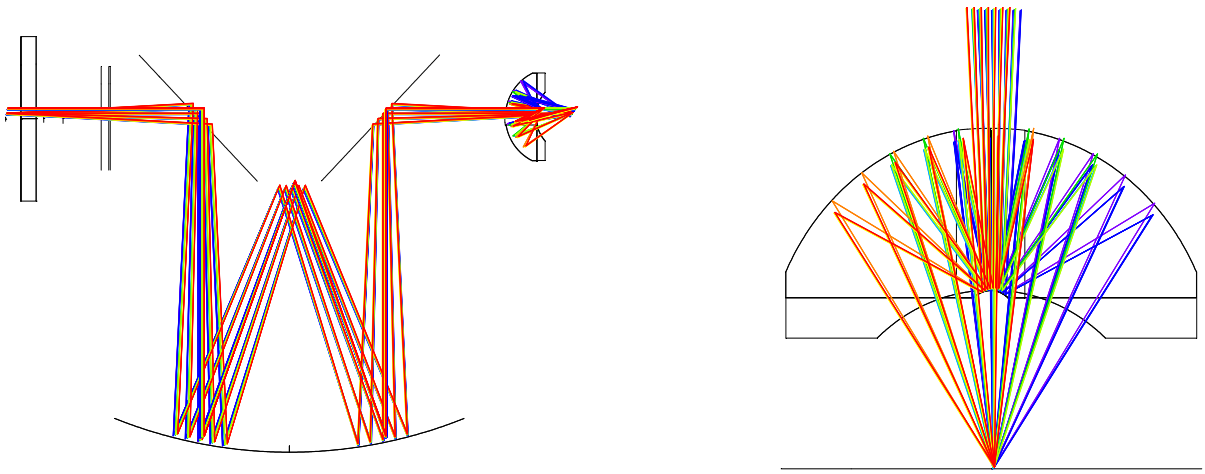

Figure2. *The ray trace diagram on the left hand side is the layout of the Offner relay 1:1 reimaging system in conjunction with a ZnS f/1.5 focal reducer. On the right is a close up view of the focal reducer.*

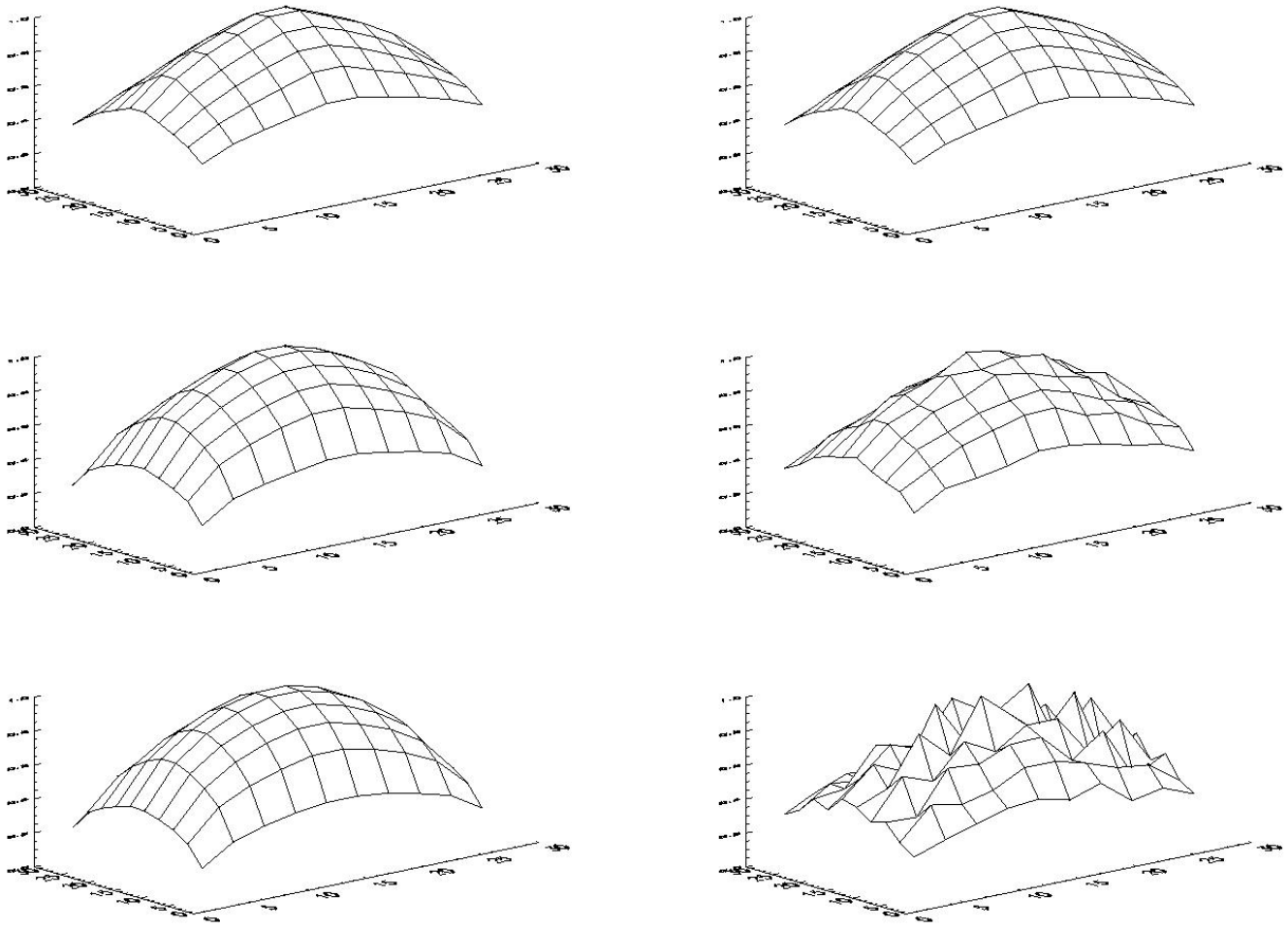

Figure 1. The credibility of the numerical solution of the IPS depends upon the width of the PSF. In these simulations, the cross pixel response was assumed to be zero, and the size of the pixel we used for simulation was 27 μ m. An IPS function and a gaussian PSF was assumed, and used to simulate the signal response function (including the contribution of noise terms, like poisson noise etc.), which was subsequently used to retrieve the original IPS function. Note that this method works well for highly undersampled PSF's. From top-to-botton on the left are the simulated signal response functions for PSF's having full width half maxima (FWHM) of 1.67 μ m, 5 μ m, and 6.7 μ m, respectively, whereas the respective figures on their right are the numerically retrieved IPS functions. We can see in the figure that as the PSF increases the IPS function obtained gets more and more erratic.

4.1 EXPERIMENT STRATEGY

The most crucial part of our experiment is to obtain a highly undersampled image, whose width is limited by the diffraction of the optical system, i.e. through diffraction, design residuals, fabrication, and alignment errors. We need to have a pinhole of the optimum size, big enough to let in enough light, but much smaller than the image size produced by diffraction. Further, the beam coming out of the pinhole should be faster than the f/10 beam for the best focusing

performance of the optical system. The smallest spot size which can be obtained, after optimum focusing, can be approximately estimated by using the following quadrature sum formula :

$$D_{eff} = \sqrt{D_{ph}^2 + D_{diff}^2 + D_{fe}^2}$$

where D_{eff} is the size of the spot, D_{ph} (physical pinhole size x 1/7) is the geometrical size of the pinhole, D_{diff} (= 1.22* λ *f/# = 1.83* λ) is the diffraction limited size of a point source, and D_{fe} is the spot size due to the optical realization. For longer wavelengths, the spot size is limited by the diffraction (ref. to Table 1). The optical errors should contribute from 2 microns (based on Monte Carlo analysis) to 4 microns (based on RSS'ing the errors from each tolerance assuming the tolerance was just met) of image size. One of the most crucial things for obtaining the sharpest focus is to have the correct distance between the focal reducer and the plane of the detector - even a slight offset of a few hundred microns will result in an out of focus spot.

The first step in our experiment is to locate the pinhole image on the detector and move it to the center of the circular field of the region imaged by the focal reducer. The imaging of the focal reducer is best in a very small region of 10x10 pixel area, and we were able to see the deterioration in the image quality as we the pinhole image from the center of the focal reducer. Once we are able to move the spot to the center of the focal reducer, we run a code to find out the position of the best focus by moving the pinhole along the z axis and analyzing the images as a function of this piston. To meet high precision requirements, we also developed a code, which could find out the relative tilt between the detector plane and the axes of the translational stage. And finally to take a 10x10 exposures over a single pixel in a grid like manner, by moving the pinhole in such a manner that it is always in the object focal plane (using the information obtained for detector tilt). And the signal response function thus obtained could be used to derive the IPS function by using a calculated PSF as discussed in the section 3.

Table 1. This table has the calculated theoretical limits of the the size of the PSF for various sizes of pinholes at different wavelengths. The effects of diffraction, object size, and optical error (~2 microns) have been considered.

Pinhole Sizes (in microns)	Calculated spot size (in microns) for λ = 1 μ m	Calculated spot size (in microns) for λ = 2 μ m	Calculated spot size (in microns) for λ = 3 μ m	Calculated spot size (in microns) for λ = 4 μ m	Calculated spot size (in microns) for λ = 5 μ m
25	4.63	5.61	6.94	8.46	10.08
10	3.10	4.43	6.03	7.73	9.48
5	2.81	4.23	5.89	7.62	9.39

4.2 PRELIMINARY EXPERIMENTAL RESULTS

We were able to implement our automated codes to find out the best focus, and to take exposures while scanning a region of 2x2 pixels in a grid like manner (25 samples per pixel) to obtain the signal response as a function of spatial position of the center of the spot. However we were unable to obtain a highly undersampled image, the most crucial

requirement of our experiment. We used a J band filter whose central wavelength is around 1.25 μm, and a 10 μm pinhole. The best possible focus produce an image that was just critically sampled and elliptical in structure (Fig. 3). We used Zemax simulations to determine that the elliptical, and bigger, spot size were due to an offset of the detector plane from the ideal focal plane position.

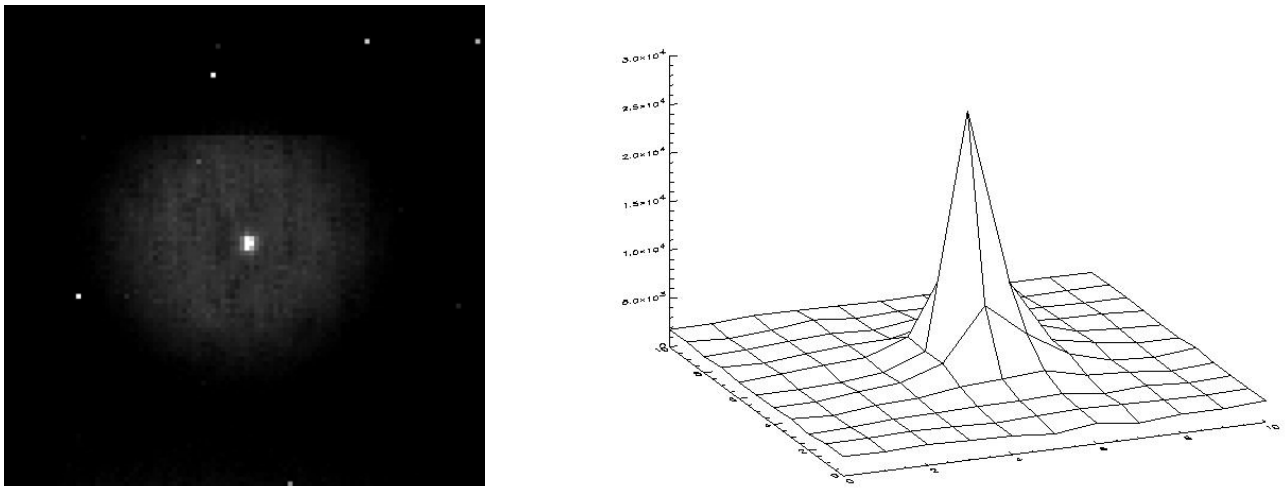

Figure 3. On the left is the critically sampled image of the 10 micron pinhole. On the right is the structure of the same image. We can see that the PSF is roughly a pixel wide, which implies it is just critically sampled. Further we can notice that it is asymmetric in its structure.

5. LIMITATIONS OF THE EXPERIMENT

The IPS experiment requires extremely high precision measurements and hence its accuracy is affected by many variables. The position of the detector plane with respect to the focal reducer is very crucial, and even a shift of $\pm 125 \mu m$ from the ideal position may lead to an optical spot considerably out of focus. Unfortunately, we do not have a mechanism for readjusting the distance between the focal reducer and the detector plane, due to complications involved in implementing a highly precise, and movable, detector mount inside the dewar, at cryogenic temperatures. Another variable that might affect the spot size is the magnitude of mechanical vibrations in the system. While these would be minimized by using the optical air table, there are still some vibrations induced by the cryogenic cooling pump. However from the calculation of the center of mass of a spot in a set of multiple exposure images, it was found that the order of error due to these vibrations is definitely less than half a micron. Such an effect is negligible for all case under consideration.

6. CONCLUSION

The IPS experiment in the IDTL has shown promising results, with almost all the codes working fine in order to carry out the experiment. We were able to run and test our experiment with the critically sampled spot we obtained. However, the precision of our results depend upon our ability to obtain a highly undersampled spot (<5 microns). For that we plan to obtain a detector whose surface has been precisely metered with respect to its mount, hence enabling us to minimize the offset of the detector plane from its ideal position (i.e., the focal plane of the focal reducer). We also plan to study the wavelength dependence of IPS variations in later stages.

7. ACKNOWLEDGEMENTS

The material based in this paper is based upon work supported, in part, by NASA, under award No. NAG5-10430.

8. REFERENCES

1. Anderson J., and King I.R., "Toward high-precision astrometry with WFPC2. I. Deriving an accurate point spread function," P.A.S.P. **112**, 1360-1382 (2000)
2. Holtzman, J. A., "The Performance and Calibration of WFPC2 on the Hubble Space Telescope," P.A.S.P. **107**, 156-178 (1995).
3. Lauer T. R., "Combining undersampled dithered images," P.A.S.P. **111**, 227-237 (1999)
4. Lauer T. R., "The photometry of undersampled point-spread functions," P.A.S.P. **111**, 1434-1443 (1999)
5. Kavaldjiev D., and Ninkov Z., "Subpixel sensitivity for a charge-coupled device," Opt. Eng. **37**(3), 948-954 (1998)
6. Kavaldjiev D., and Ninkov Z., "Influence of non-uniform CCD pixel response on aperture photometry," Opt. Eng. **40**(2), 162-169 (2001)
7. Piterman A., and Ninkov Z., "Subpixel sensitivity for a back illuminated charge-coupled device and the effects of non-uniform response on measurement accuracy," Opt. Eng. **41**(6), 1192-1202 (2002)
8. Levy D., Schacham S. E., and Kidron I., "Three-dimensional analytical simulation of self responsivities of photovoltaic detector arrays," IEEE Trans. Electron Devices **ED-34**(10), 2059-2070 (1987)
9. Figer D. F. etal., "The Independent Detector Testing Laboratory and the NGST Detector Characterization Project," SPIE Proceedings (to be published)
10. R.P. Kanwal, "Linear Integral Equations", 2nd ed., Birkhauser, Boston (1997)
11. G. Evans, "Practical Numerical Analysis", Wiley, New York (1995)